NUMERICAL STUDY OF PERFORATED PLATE CONVECTIVE HEAT TRANSFER

by

Mladen A. TOMIĆ [a*], Predrag Z. ŽIVKOVIĆ [b], Mića V. VUKIĆ [b], Gradimir S. ILIĆ [b], and Mladen M. STOJILJKOVIĆ [b]

[a] College of Applied Technical Sciences, Nis, Serbia
[b] Faculty of Mechanical Engineering, University of Nis, Nis, Serbia

Original scientific paper
DOI: 10.2298/TSCI1403949T

Numerical simulations were performed to determine the heat transfer coefficient of a perforated plate with square arranged cylindrical perforations. Three parameters were varied in the study: plate porosity, pitch Reynolds number and working fluid, while perforation diameter and plate thickness were constant. The Reynolds number was varied in the range from 50 to 7000, and porosity in the range from 0.1 to 0.3. As working fluids, helium, air or carbon-dioxide were set, respectively. The Nusselt number was correlated in the function of the Reynolds number, the Prandtl number, and the pitch-to-diameter ratio. The comparison with other correlations is given at the end of the paper. The difference was found to be acceptable.

Key words: *heat transfer, perforated plate, porosity, numerical simulation, heat exchanger*

Introduction

One of the most important properties of heat exchangers, apart from having high effectiveness, is the need to be very compact, *i. e.* they must accommodate a large amount of surface to volume ratio. This helps reduce the heat loss to the surroundings by reducing the exposed surface area. Smaller mass also means smaller heat inertia, *i. e.* faster cooling time for refrigeration. This requirement is particularly important for small refrigerators operating at the liquid helium temperature. Several types of cryogenic heat exchangers have been reviewed by Dilevskaya [1]. The need to attain high effectiveness and high level of compactness together in one unit led to the invention of the matrix heat exchanger (MHE) by McMation *et al.* [2]. The matrix heat exchanger consists of a package of perforated plates with a multitude of flow passages aligned in the direction of flow allowing high heat transfer in a properly designed unit (fig. 1). These exchangers can have up to 6000 m^2/m^3 surface to volume density [3].

In 1966 an extensive experimental study of convective heat transfer and flow friction based on transient technique was published for eight different perforated surfaces [4]. In the report, the authors concluded that the perforations of perforated plate heat exchangers apparently disturb the thermal boundary layer to a much higher degree than the hydrodynamic boundary layer. According to the authors, by using perforated materials, an improvement in heat transfer was made.

* Corresponding author; e-mail: tomicmladen@yahoo.com

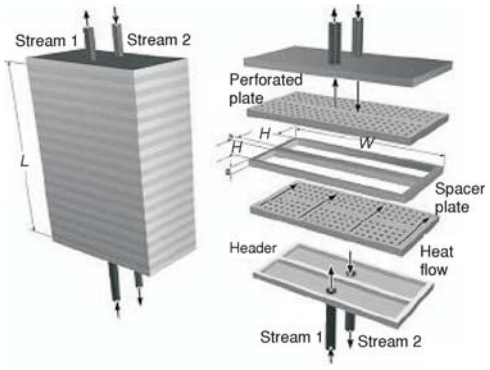

Figure 1. Matrix heat exchanger schematic [4]

A proper literature review could be found in the papers of Venkatarathnam and Moheisen´s report [5, 6]. According to their research, perforated plates and fins find a large field of application in different heat exchangers, film cooling, and solar collectors [7-12].

The goal of this research is to determine the heat transfer coefficient for the 2 mm thin square arranged perforated plate. The porosity σ, which represents the ratio of open area over total surface, was varied from 0.1 to 0.3, and the pitch based Reynolds number between 100 and 10000, while the hole diameter was kept constant.

Literature review

Heat transfer improvement may generally be achieved by increasing the heat transfer coefficient, heat transfer surface areas, or both. In papers [13-15] the authors have concluded that for certain values of the perforation dimension, a perforated plate enhances heat transfer in comparison to a solid plate. The perforated plate convective heat transfer takes place on three surfaces: the front area surface, the tubular surface of the perforation, and the back surface of the plate. Brunger *et al.* [16] studied the effectiveness for each of the three zones of heat transfer on a perforated plate. In their study, they considered large pitch to diameter ratios (>6.67). For each of the heat transfer regions, an equation for effectiveness was given. The authors also stated that under typical operating conditions, about 62% of the ultimate rise of the air temperature was predicted to occur on the front surface, 28% in the hole, and 10% on the back of the plate. An average heat transfer for the plate may be defined as:

$$\alpha = \frac{\sum_{i=1}^{n} \alpha_i A_i}{\sum_{i=1}^{n} A_i} \tag{1}$$

The flow through the tubular section could be considered as the developing flow with a very high heat transfer coefficient. The heat transfer coefficient in the developing flow is well studied, and it can be calculated as the function of the product of the Reynolds and the Prandtl number in the following form [17]:

$$\alpha = \zeta 0.0465(\mathrm{Re\,Pr})^{0.75} \frac{\lambda}{d} \tag{2}$$

where ζ is the function of tubular perforation length L and the length needed for the fully developed flow L'. The length L' is equal to:

$$L' = 0.015\mathrm{RePr}d \tag{3}$$

The ζ value dependance is presented in tab. 1.

Table 1. The ζ value dependance

L/L'	0	0.01	0.05	0.1	0.2	0.4	0.6	0.8	1.0	∞
ζ	∞	1.26	1.16	1.12	1.08	1.05	1.03	1.01	1.00	1.00

Linghui *et al.* [18] studied the flow through hexagonally arranged perforations on the plate. The purpose of the research was to determine how the plate thickness and perforations diameter ratio (δ/d) affected the heat transfer coefficient. They studied ratios varying from 0.333 to 1.1666, holding the diameter constant while plate thickness was varied. Their experiments used the naphthalene sublimation technique to determine the heat transfer of the plate. The research led to the conclusion that there was little change in the heat transfer coefficients between the (δ/d) ratios of 0.5 and 1.1. The final equation for the Nusselt number inside the tube was:

$$\mathrm{Nu} = 2.058\mathrm{Re}^{0487} \tag{4}$$

The heat transfer from the front face of the plate was studied by Sparrow and Ortiz [19]. In their experiments Reynolds number and the perforation's pitch to diameter ratio was varied. The suggested Nusselt criterion was a function of the Reynolds and Prandtl number, and the characteristic length in the Nusselt criterion was the ratio of module surface area to the pitch:

$$\mathrm{Nu} = 0.881\mathrm{Re}^{0.476}\mathrm{Pr}^{1/3}, \quad 2000 < \mathrm{Re} < 20000 \tag{5}$$

and

$$\mathrm{Nu} = \frac{\alpha A}{\lambda p} \tag{6}$$

The result was established for the limited case, where relative spacing is $2 < p/d < 2.5$. Dorignac *et al.* [20] conducted a series of experiments of air flow leading to the result for the Reynolds number of 1000 to 1200:

$$\mathrm{Nu} = 1.202\left(\frac{p}{A^{0.5}}\right)^{1.879}\left(\frac{p}{d}\right)^{0.163}\mathrm{Re}^{0.409} \tag{7}$$

where p is the pitch length and A is the area. Heat transfer rate in the back face of the last plate is high due to flow separation and the resulting turbulence [19]. The Nusselt number correlation as a function of the Reynolds number, the Prandtl number and the geometry factors are generally applicable to higher Reynolds numbers and lower plate porosities. Many authors have derived empirical correlations for the Nusselt number and friction factor *vs*. the Reynolds number. The general approach was to find the relation in the form:

$$\mathrm{Nu} = C\mathrm{Re}^{n} \tag{8}$$

where C and n are the functions of geometric parameters. A good review of these functions can be found in [3, 5, 6]. Ornatskii *et al*. [21] gave the expression in the form as in eq. (8) where constant C and exponent n are calculated as:

$$C = 4.9\sigma - 0.11 \tag{9}$$

and

$$n = 0.77 - 1.12\sigma \tag{10}$$

Andrews and Bazdidi-Teherani presented in their paper the correlation of diameter-based Nusselt number *vs*. the product of powers of pitch-to-diameter and diameter based Reynolds number [22]. The correlations equivalent in the form of pitch is:

$$\mathrm{Nu} = 9.07\left(\frac{p}{d}\right)^{-0.1317}\mathrm{Re}^{0.2523} \tag{11}$$

The equation was valid for pitch-to-diameter ratio between 4.7 and 21. Kutsher [23] conducted a series of experimental and numerical studies for low-porosity plates and gave a correlation in the similar form as Andrews and Bazdidi-Teherani [22]. The Nusselt criteria was determined as:

$$\mathrm{Nu} = 2.867\left(\frac{p}{d}\right)^{0.221} \mathrm{Re}^{0.4295} \tag{12}$$

Andrew *et al.* [24] developed a model to determine the convective heat transfer coefficient of the upstream face, tubular perforations and the leeward face of a perforated plate using computational fluid dynamics (CFD). The plate's perforations were modeled as hexagonally shaped flow patterns, which is similar to Sparrow's model presented earlier [25]. The data obtained from the CFD model were found to agree within a few percent of Sparrow's data. This led to the conclusion that the CFD model and solution were valid. The final Nusselt number equation for the front side of a perforated plate, at $2000 \leq \mathrm{Re} \leq 20000$, was presented as:

$$\mathrm{Nu} = 1.057\mathrm{Re}^{0.457}\mathrm{Pr}^{0.333} \tag{13}$$

The model was applied to the tubular surface of the perforations and the leeward side of the perforated plate to determine their effect on the overall convective heat transfer coefficient of the matrix heat exchanger. The results showed that the plate thickness had a substantial influence on the amount of heat transfer occurring within the tubular part of a matrix heat exchanger, and that the leeward side of the perforated plate required more detailed investigation. In conclusion, the equation for the Nusselt number for fluid flow as a function of the Reynolds number was presented, taking into account the convection at the front, the back, and at the tubular perforations, in the plate as:

$$\mathrm{Nu} = 0.445\mathrm{Re}^{0.607}\mathrm{Pr}^{1/3} \tag{14}$$

or for air when $\mathrm{Pr} = 0.707$ as:

$$\mathrm{Nu} = 0.397\,\mathrm{Re}^{0.607} \tag{15}$$

Mathematical model

In order to obtain the most suitable model, several models were tested: standard k-ε, low-RE k-ε, RNG k-ε, and k-ε model. Although all of them gave similar results, except the k-ε model which diverged, the RNG k-ε model presented itself as the fastest converging, and therefore was adopted for the simulation (fig. 2). This could be expected, because the RNG k-ε model proved to be suitable for the calculation of a number of separated flows, and it is this version of the model that has been provided in the PHOENICS software.

The mathematical model is based on:

– continuity equation

$$\frac{\partial(\rho)}{\partial t} + \frac{\partial}{\partial x_i}(\rho u_i) = 0 \tag{16}$$

– momentum (Navier-Stokes) equations

$$\frac{\partial(\rho u_i)}{\partial t} + \frac{\partial}{\partial x_j}(\rho u_i u_j) = \frac{\partial}{\partial x_j}(\tau_{ij}) - \frac{\partial p}{\partial x_i} + f_i \tag{17}$$

– energy equation

$$\frac{\partial(\rho h)}{\partial t} + \frac{\partial}{\partial x_i}(\rho u_i h) = \frac{\partial}{\partial x_i}(j_{ih}) + S_h \tag{18}$$

where ρ is the density, u_i – the three main velocity components, p – the pressure, f_i are the body forces and any other additional momentum sources, h is the enthalpy, and S_h represents the generation/destruction rate of enthalpy. The t_{ij} is the momentum shear stress tensor, and the j_{ih} – the diffusion flux of energy transport. In the energy equation, the diffusion flux of energy transport term j_{ih} includes the energy transfer due to conduction, species diffusion and viscous dissipation:

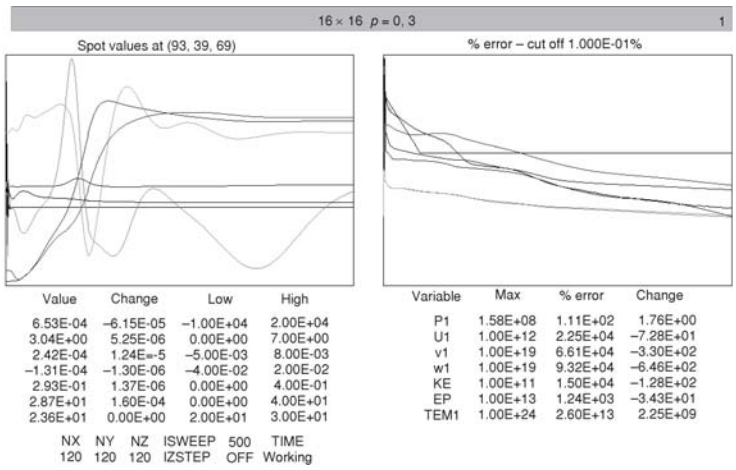

Figure 2. An example of obtained convergence for the RNG *k-ε* model

$$j_{ih} = \Gamma_T \frac{\partial h}{\partial x_i} - \sum_j h_j j_{jc} + \Phi \tag{19}$$

where the factors Γ_T are the diffusion coefficients for the enthalpy (Fourier's law).

The second term on the right hand side in eq. (18) represents the energy transport by diffusion of species and the Soret-effect species diffusion transport, respectively. Finally, the term Φ is the viscous dissipation defined as:

$$\Phi = 0.5\mu\left(\frac{\partial u_i}{\partial x_j} + \frac{\partial u_j}{\partial x_i}\right)^2 - \frac{2}{3}\mu\frac{\partial u_k}{\partial x_k}\frac{\partial u_l}{\partial x_l} \tag{20}$$

As the former equations represent the system averaged equations, it was needed to implement a turbulent model in order to close the system and to convert the given set of differential equations into algebraic, which were solved using the PHOENICS software package.

Numerical setup

In the study, a plate with 16×16 perforations was placed in the numerical channel (fig. 3). The plate was set to be the constant temperature heat source, similar to assumptions made by Sparrow [19]. The fluid stream consisted of either helium, air or carbon-dioxide, and was set to flow perpendicularly to the plate. In order to generate the optimal grid, the grid size was varied in two directions along plate length and width, regarding the Y-Z plane. The grid was set to square in the Y-Z plane (fig. 3). The length of the cell in these two directions was varied from 0.88 to 0.2 mm, while the fluid temperature on the outlet was chosen as a quality parameter. The results showed that under the cell size of 0.8 mm, the temperature on the outlet was

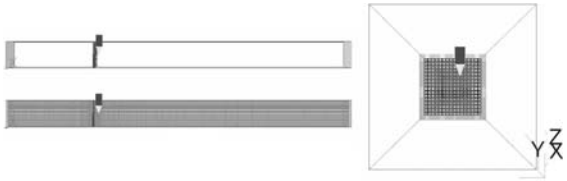

Figure 3. Numerical channel and grid in x-direction (left) and front view (right)

varying not more than 0.1 K (tab. 2.). According to this, the cell length was chosen to be 0.5 mm, *i. e.* 4 cells per hole diameter.

Table 2. Outlet temperature variation in the function of cell size

Cell size [mm]	0.878	0.798	0.721	0.598	0.527	0.351	0.263
Outl. temp. [°C]	21.65	22.3	22.28	22.33	22.35	22.22	22.4

The energy balance for the fluid side is represented as:

$$\dot{Q} = \dot{m} c_p \Delta t \tag{21}$$

i. e.,

$$\dot{Q} = \rho u A c_p (t_{\text{out}} - t_{\text{in}}) \tag{22}$$

where c_p represents the mass specific heat capacity and u is the fluid velocity. The heat transmitted from the plate is equal to:

$$\dot{Q} = \alpha F \Delta\theta \tag{23}$$

i. e.

$$\dot{Q} = \alpha F (t_{\text{pl}} - t_{\text{in}}) \tag{24}$$

where F represents the active heat transfer surface (the sum front surface of a plate, the back surface of a plate and the inner surface of perforations), and $\Delta\theta$ is the difference between the plate surface temperature and the inlet fluid temperature. Combining eq. (22) and (24), the heat transfer coefficient is then equal to:

$$\alpha = \frac{\rho u A c_p (t_{\text{out}} - t_{\text{in}})}{F (t_{\text{pl}} - t_{\text{in}})} \tag{25}$$

Results and discussion

For the Nusselt criterion an arbitrary function was chosen according to eq. (11), expanded by the Prandtl number function:

$$\text{Nu} = a \left(\frac{p}{d} \right)^k \text{Re}^n \, \text{Pr}^m \tag{26}$$

The term (p/d) of eq. (26) on the right-hand side is inverse proportional to the square root of the porosity α and therefore represents the influence of the porosity on the heat transfer. The Reynolds number was defined as the function of the free stream fluid velocity:

$$\text{Re} = \frac{up}{\nu} \tag{27}$$

and the Nusselt number is equal to:

$$\text{Nu} = \frac{\alpha p}{\lambda} \tag{28}$$

The characteristic length in Reynolds and Nusselt number p represents the pitch of the plate, which is a characteristic of the plate and therefore represents all surfaces involved in the heat transfer. Finally, after the fitting, the Nusselt criterion was found to be:

$$\text{Nu} = 0.09 \left(\frac{p}{d} \right)^{0.137} \text{Re}^{0.527} \, \text{Pr}^{-5.66} \tag{29}$$

with regression of 0.96. Figures 4 and 5 show a comparison of the pitch based Nusselt number for the currently obtained relation and different criteria equations obtained by Ornatskii *et al.* [21], Andrews and Bazdidi [22], Kutscher [23], and Andrew *et al*. [24]. The results are presented in figs. 4 and 5 for the plate porosity of 10% and 30%, respectively. The first thing that can be noted both in figs. 4 and 5 is the high difference for the results obtained from Kutscher's [23] and Andrews and Bazdidi [22] relations. The reason is in the fact that those two relations refer to plates with low porosity, therefore higher pitch to diameter ratios. On the other side, three relations developed by Ornatskii *et al*. [22], Andrew *et al.* [24] and the current research results are grouped. As it can be seen from the figures, those three relations show high mutual agreement.

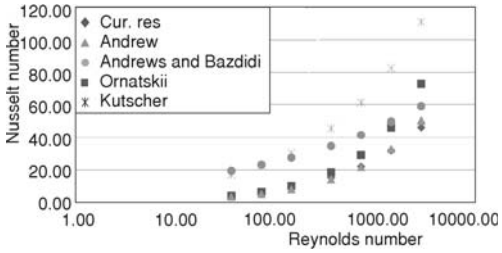

Figure 4. Comparison of results for air flow through 10% porous plate

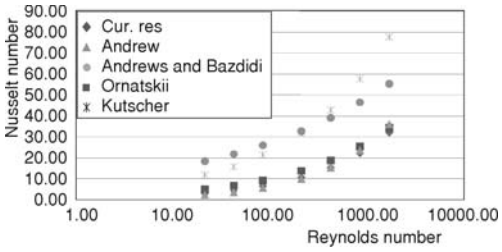

Figure 5. Comparison of results for air flow through 30% porous plate

Conclusion

Through the use of a model of porous plate media and assuming the constant temperature condition, a model for heat transfer was developed and verified against the research of other authors. The Nusselt criterion was obtained for a wide range of parameters, when porosity is in the range from 0.1 to 0.3, and for the Reynolds number between 50 and 7000. The results show good agreement with the existing Nusselt correlations in the case of air flow.

Nomenclature

A – module surface, [m^2]
d – perforation diameter, [m]
F – total surface, [m^2]
L – length, [m]
L' – length needed for flow to fully develop, [m]
Nu – Nusselt number
p – pitch, [m]
Pr – Prandtl number
Re – Reynolds number
t – temperature, [°C]
u – fluid velocity, [ms^{-1}]

Greek symbols

α – heat transfer coefficient, [Wm^{-2}K^{-1}]
λ – thermal conductivity, [Wm^{-1}K^{-1}]
ν – kinematic viscosity of the fluid, [m^{2}s^{-1}]
ρ – density of the fluid, [kgm^{-3}]
σ – plate porosity, [–]

Subscripts

in – inlet
out – outlet
pl – plate

References

[1] Dilevskaya, A., *Micro Cryogenic Heat Exchangers* (in Russian), Mashinostrenie, Moscow, 1978
[2] McMahon, H. O., *et al.*, A Perforated Plate Heat Exchanger, *Trans ASME, 72* (1950), pp. 623-632
[3] Krishnakumar, K., Venkataratham, G., Transient Testing of Perforated Plate Matrix Heat Exchangers, *Cryogenics, 43* (2003), 2, pp. 101-109

[4] Bannon, J. M., *et al.*, Heat Transfer and Flow Friction Characteristics of Perforated Nickel Plate-Fin Type Heat Transfer Surfaces, Technical report no. 52, United States Naval Postgraduate School, Monterey, Cal., USA, 1965
[5] Venkataratham, G., Sarangi, S., Matrix Heat Exchangers and their Application in Cryogenic System, *Cryogenics, 30* (1990), 11, pp. 907-918
[6] Ragab, M. M., Transport Phenomena in Fluid Dynamics: Matrix Heat Exchangers and their Applications in Energy Systems, Report No. Afrl-rx-ty-tr-2010-0053, Air Force Research Laboratory Materials and Manufacturing Directorate, Tyndall Air Force Base, Panama City, USA, 2009
[7] Kakac, S., *et al*., *Heat Exchangers, Thermal-Hydraulic Fundamentals and Design*, Hemisphere Publishing Corporation, New York, USA, 1981
[8] Bergles, A. E., Technique to Augment Heat Transfer, in: *Handbook of Heat Transfer Applications* (Eds. W. M. Rohsenow, J. P. Hartnett, E. N. Ganic), Ch. 3, 2nd ed., McGraw-Hill Book Company, N. Y., USA
[9] Al-Essa, A. H., Al-Hussien, F. M. S., The Effect of Orientation of Square Perforations on the Heat Transfer Enhancement from a Fin Subjected to Natural Convection, *Heat Mass Trans, 40* (2004), 6-7, pp. 509-515
[10] Mullisen, R., Loehrke R., A Study of Flow Mechanisms Responsible for Heat Transfer Enhancement in Interrupted-Plate Heat Exchangers, *J Heat Trans., 108* (1986), 2, pp. 377-385
[11] Kutscher, C. F., Heat Exchange Effectiveness and Pressure Drop for Air Flow through Perforated Plates with and without Crosswind, *J Heat Trans., 116* (1994), 2, pp. 391-399
[12] White, M. J., *et al*., An Experimentally Validated Numerical Modeling Technique for Perforated Plate Heat Exchangers, *J Heat Transf, 132* (2011), 11, pp.1-9
[13] Al-Essa, A. H., Augmentation of Heat Transfer of a Fin by Rectangular Perforations with Aspect Ratio of Three, *Int J Mech Appl, 2* (2012), 1, pp. 7-11
[14] Al-Essa, A. H., *et al*., The Effect of Orientation of Square Perforations on the Heat Transfer Enhancement from a Fin Subjected to Natural Convection, *Heat Mass Trans, 40* (2004), 6-7, pp. 509-515
[15] Swee-Boon, C., *et al.*, Forced Convective Heat Transfer Enhancement with Perforated Pin Fins, *Heat Mass Trans*, (2013), doi 10.1007/s00231-013-1186-z
[16] Brunger, A. P., *et al*., Heat-Exchange Relations for Unglazed Transpired Solar Collectors with Circular Holes on a Square or Triangular Pitch, *Solar Energy, 71* (2001), 1, pp. 33-45
[17] Schmidt, E., *et al*., Heat Science (in Serbian), Faculty of Mechanical Engineering, University of Belgrade, Belgrade, 1971
[18] Linghui, G., *et al*., The Effect of the Geometric Parameters of a Perforated Plate on Its Heat Transfer Characteristics, *Cryogenics, 36* (1996), 6, pp. 443-446
[19] Sparrow, E. M., Ortiz, M. C., Heat Transfer Coefficients for the Upstream Face of a Perforated Plate Positioned Normal to an Oncoming Flow, *Int J Heat Mass Transf, 25* (1982), 1, pp. 127-135
[20] Dorignac, E., *et al*., Experimental Heat Transfer on the Windward Surface of a Perforated Flat Plate, *Int J Therm Sci, 44* (2005), 9, pp. 885-893
[21] Ornatskii, A. P., *et al*., Experimental Study of Perforated Plate Heat Exchanger for Micro Cryogenic System (in Russian), *Promish Teplo Tekhn, 5* (1983), pp. 28-33
[22] Andrews, G. E., Bazdidi-Teherani F., Small Diameter Film Cooling Hole Heat Transfer: The Influence of the Number of Holes, *Proceedings*, American Socienty of Mechanical Engineers Gas Turbine and Aeroengine Congress and Exposition, Toronto, Canada, 1989
[23] Kutscher, C. F., An Investigation of Heat Transfer for Air Flow through Low Porosity Perforated Plates, Ph. D. thesis, University of Colorado at Boulder, Boulder, USA, 1992
[24] Andrew, M. H., *et al*., The Thermal Modeling of a Matrix Heat Exchanger Using a Porous Medium and the Thermal Non-Equilibrium Model, *International Journal of Thermal Sciences, 47* (2008), 10, pp. 1306-1315
[25] Sparrow, E. M., O'Brien, J. E., Heat Transfer Coefficients on the Downstream Face of an Abrupt Enlargement or Inlet Constriction in a Pipe, *J Heat Transf., 10*2 (1980), 3, pp. 408-414

Paper submitted: January 21, 2014
Paper revised: March 25, 2014
Paper accepted: April 8, 2014